Energy Partition to the Workpiece for Grinding with Aluminum Oxide and CBN Abrasive Wheels

S. Kohli
Research Assistant.

C. Guo
Research Associate.

S. Malkin
Professor.
Fellow ASME

Department of Mechanical Engineering,
University of Massachusetts,
Amherst, MA 01003

An experimental investigation is reported of the energy partition to the workpiece for grinding of steels with aluminum oxide and cubic boron nitride (CBN) abrasive wheels. The energy input to the workpiece was obtained by measuring the temperature distribution in the workpiece using an embedded thermocouple technique and matching the results with analytically computed values. It was found that 60–75 percent of the grinding energy is transported to the workpiece as heat with an aluminum oxide abrasive wheel, as compared to only about 20 percent with CBN wheels. An analysis of the results indicates that the much lower energy partition to the workpiece with CBN can be attributed to its very high thermal conductivity whereby a significant portion of the grinding heat is transported to the abrasive instead of to the workpiece. The much lower energy partition to the workpiece with CBN wheels results in much lower grinding temperatures and a greatly reduced tendency for thermal damage to the workpiece.

Introduction

The grinding process requires a very high input of energy per unit volume of material removed. Virtually all this energy is converted to heat within the grinding zone, thereby leading to high temperatures and possible thermal damage to the workpiece. Heat associated with the energy expended by grinding is transported away from the grinding zone by the workpiece, the grinding fluid, the grinding chips, and the grinding wheel. Of particular interest is the fraction of the total energy transported as heat to the workpiece, which is directly related to the workpiece temperature rise.

Thermal analyses of grinding are usually based on classic moving heat source theory (Jaeger, 1942). The temperatures calculated are generally found to be proportional to the product of the total energy expended and the fraction of this energy entering the workpiece as heat (Malkin, 1989 and Snoeys et al., 1978). Maris and Snoeys (1973) concluded from a critical review of the literature that 60 percent to 90 percent of the grinding energy is transported as heat to the workpiece with aluminum oxide wheels, although the only direct experimental evidence cited was that of Sato (1961) and Malkin (1968). This is also consistent with experimental results subsequently reported by Malkin and Anderson (1974) who used a calorimetric method to measure the energy partition to the workpiece.

As compared to grinding with conventional aluminum oxide wheels, thermal damage with cubic boron nitride (CBN) superabrasive wheels is generally much less of a problem (Malkin, 1985). For grinding of steels with CBN wheels, workpiece burn rarely occurs, and residual stresses are found to be predominantly compressive (Tönshoff and Grabner, 1984; Tönshoff and Hetz, 1985 and Vansevenant, 1989). This indicates lower grinding temperatures with CBN than with aluminum oxide wheels. Lower temperatures with CBN may be partly due to lower energy requirements, but it has been postulated that the main effect can be attributed to the very high thermal conductivity of CBN whereby a much larger fraction of the grinding heat is transported to the abrasive instead of to the workpiece (Lavine, Malkin and Jen, 1989). However, no experimental energy partition results have been reported up to now for grinding with CBN.

The present investigation was undertaken to experimentally determine and compare the energy partition to the workpiece for grinding with aluminum oxide and CBN abrasive wheels. For this purpose, the grinding temperature distribution in the workpiece was measured from which the energy input to the workpiece was analytically calculated by matching the computed temperature to the measured temperature. The energy partition was then obtained by dividing the energy input to the workpiece by the measured net grinding energy.

Experimental

Straight surface grinding experiments were conducted using aluminum oxide and CBN wheels under plunge conditions as illustrated in Fig. 1. The temperature distribution in the workpiece was measured using an embedded thermocouple. The total grinding power at the wheel spindle was measured using a Hall effect transducer (F.W. Bell-PX 2202B) from which the net power was obtained by subtracting the measured idling power. In an initial series of tests, the net power obtained in this way was found to be virtually identical to that obtained

Contributed by the Production Engineering Division for publication in the JOURNAL OF ENGINEERING FOR INDUSTRY. Manuscript received Jan. 1993; revised March 1994. Associate Technical Editor: A. Lavine.

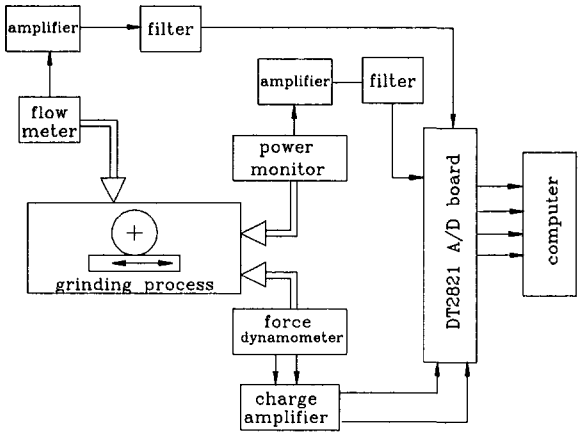

Fig. 1 Experimental setup for temperature measurements

from force measurements using a dynamometer (Kistler 9275A). The thermocouple and the power transducer were interfaced to a personal computer (PC) for data collection and analysis.

The embedded thermocouple technique which was adopted is similar to that used by Littmann and Wulff (1955), Takazawa (1966), and Sauer (1971). The temperature response is measured during successive passes of the grinding wheel over the workpiece. The pass at which the thermocouple is ground and destroyed provides a reference for calculating the depth below the surface for the temperature measurements during the previous grinding passes. The thermocouple was welded to the workpiece through a hole as illustrated in Fig. 1. A type K chromel-alumel (30 gage wire) thermocouple was selected for temperature measurements which has a recommended temperature range of -165 to 1260°C. Each wire of the thermocouple has a diameter of 0.254 mm and the two wires together are coated with teflon. The hot junction was formed by capacitive discharge welding of the two wires at the bottom of a 1.27 mm hole from the underside of the workpiece. The cold junction was immersed in a flask of ice. While it is desirable to keep the size of the thermocouple as small as possible to enhance its response, thermocouple wire smaller than 0.254 mm in diameter was found to be very difficult to weld. Furthermore, the objective was only to measure the "background" temperature distribution in the workpiece subsurface and not flash temperatures at individual cutting points, so very small thermocouples were not needed.

Experiments were performed on plain carbon steel (AISI 1020, HRB 40), hardening bearing steel (AISI 52100, HRC 62), and hardened die steel (AISI 01, HRC 62). These materials have very similar thermal properties: thermal conductivity k = 60.5 W/mK and volumetric specific heat $\rho c = 3.4 \times 10^6$ J/m^{3}K. All workpiece specimens were 100 mm long and initially 25 mm in height. The AISI 1020 and AISI 52100 specimens were 10 mm wide and the AISI 01 specimens 9.5 mm wide. Each workpiece had a hole for the thermocouple wire, as mentioned above, which was drilled in two stages. A larger 2.38 mm diameter pilot hole was first drilled from the underside of the workpiece to a depth of approximately 17.5 mm followed by a finer hole of 1.27 mm diameter for an additional nominal depth of 5.8 mm (see Fig. 1). When welded in place at the bottom of the hole, the thermocouple is approximately 1.7 mm from the top surface of the workpiece to be ground. A slot was provided on the underside of the workpiece for passage of the thermocouple wire. Machining of the hole and slot on the hardened steel workpieces was done in their normalized state prior to hardening. Subsequent heat treatment left traces of salt within the hole which had to be cleaned out prior to welding the thermocouple in place. Grinding experiments were performed with one vitrified aluminum oxide wheel (38A60I8VBE) and two CBN wheels, one vitrified (B150L100VZ) and one electroplated (100CBN). The wheels were all of diameter d_s = 250 mm and width b = 19 mm. Only the middle part of each wheel corresponding to the 9.5 to 10 mm workpiece width was used for grinding.

Prior to grinding, the aluminum oxide wheel was dressed with a single point diamond using a dressing lead s_d = 0.14 mm and radial dressing depth a_d = 0.013 mm. The CBN wheels were conditioned by grinding on a hardened T1 tool steel until the measured power reached a steady state value. The CBN wheels were also periodically dressed during the test with aluminum oxide dressing sticks. All the experiments were performed under up-grinding conditions with the wheel and workpiece velocities in opposite directions at the grinding zone. During testing, a grinding fluid consisting of a 5 percent solution of heavy duty soluble oil in water was applied. The wheel velocity was v_s = 30 m/s, the nominal workpiece velocity v_w = 8.6 m/min, and the wheel depth of cut a = 0.025 mm. The actual workpiece velocity was obtained by measuring the time duration for a single grinding pass from the power measurement. Due to difficulties in precisely controlling the hydraulic table drive of the machine, measured workpiece velocities deviated from test to test by as much as 8 percent from the nominal value. Measured workpiece velocities were used for all calculations.

The test procedure was as follows. A few initial grinding passes were taken while monitoring the power until the initial transient associated with machine deflection ended, as indicated by stabilization of the measured grinding power from pass to pass. The grinding test was then begun and all the temperature and power data were recorded and stored. After every grinding pass, the wheel was raised and then lowered again using the downfeed control on the machine without stopping and restarting the hydraulic workpiece drive in order to maintain a constant workpiece velocity throughout each test from pass to pass. A wait of a few minutes between successive grinding passes allowed the workpiece to cool until no further change in temperature could be detected. The grinding test was continued until the grinding pass which knocked off the thermocouple as indicated by a break in the thermoelectric circuit. This downfeed location was then taken for reference as zero depth, and the temperature data collected in the previous passes gave the temperature distributions at different depths below the workpiece surface calculated as the product of the number of passes before the final one and the wheel depth of cut a.

Results and Analysis

The first experiment was conducted with the aluminum oxide wheel on an AISI 1020 steel workpiece to test the overall approach. For each grinding pass the net grinding power P was measured from which the total average heat flux q at the grinding zone was obtained as

$$q = \frac{P}{l_c b} \tag{1}$$

where l_c is the grinding zone length taken as equal to the geometric contact length ($l_c = (d_s a)^{1/2}$) and b is the width of cut. For this total average heat flux, the quasi-steady state temperature distribution, $\theta_{z,x}$, at depth z in the workpiece was then calculated using moving heat source theory (Jaeger, 1942) as:

$$\theta_{z,x} = \frac{\epsilon q}{\pi k} \int_{-l}^{l} e^{\frac{-v_w(x-x')}{2\alpha}} K_0\left\{\frac{v_w}{2\alpha}\left[(x-x')^2 + z^2\right]^{1/2}\right\} f(x')dx' \tag{2}$$

where ϵ is the fraction of the total energy conducted as heat to the workpiece, $f(x')$ is the distribution function for the heat flux, K_0 is the modified Bessel function of the second kind of

order zero, and k and α are the thermal conductivity and diffusivity of the workpiece. Both rectangular (uniform) and triangular heat flux distributions as shown in Fig. 2 are commonly used for calculating grinding temperatures. Using either distribution leads to results for the maximum surface temperature which differ by only 6 percent, but the temperature distributions in the subsurface are somewhat different. A triangular heat source distribution ($f(x') = (x' + l)/l$) would seem to be more realistic since the removal rate increases proportionally along the grinding zone from the trailing edge to the leading edge. Snoeys, Peters and Maris (1978) also found better correlation between measured and calculated temperatures using such a triangular heat source.

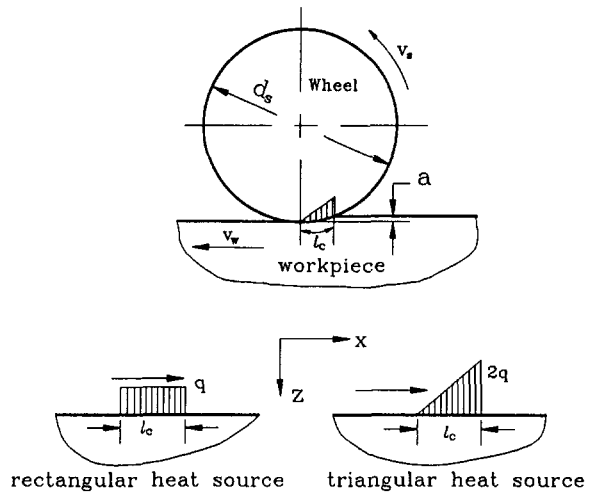

Fig. 2 Illustration of plunge grinding and heat flux distributions

Some of the measured temperatures and theoretical results for the triangular heat source at various depths (0.05, 0.1, 0.3, 0.5 mm) are shown in Fig. 3. The dimensionless length x/l along the abscissa in each graph is used to express the quasi-steady state temperature profile at any instant relative to the location of the heat source (grinding zone). The mid-point of the heat source is located at $x/l = 0$. During the experiment, the temperature is obtained as a function of distance and time, and then converted to dimensionless length according to the relationship:

$$\frac{x}{l} = \frac{x_0}{l} - \frac{v_w t}{l} - 1 \tag{3}$$

where t is the time, $2l$ the grinding zone length, x_0 the distance of the thermocouple hole from the beginning of the grinding pass, and v_w the workpiece velocity. Because the data acquisition system could not be triggered with sufficient accuracy relative to the location of the thermocouple, the measured temperature for each pass was shifted along the x-axis to better match the theoretical temperature.

For the results shown in Fig. 3, the measured temperature appears to rise slower than theoretically predicted, which suggests a time delay in the response of the temperature measuring system. In order to take this effect into account, the time constant of the system was evaluated and the theoretical temperature then modified considering the time delay before being compared with the measured temperature. For evaluating the time constant, the temperature measuring system was modeled

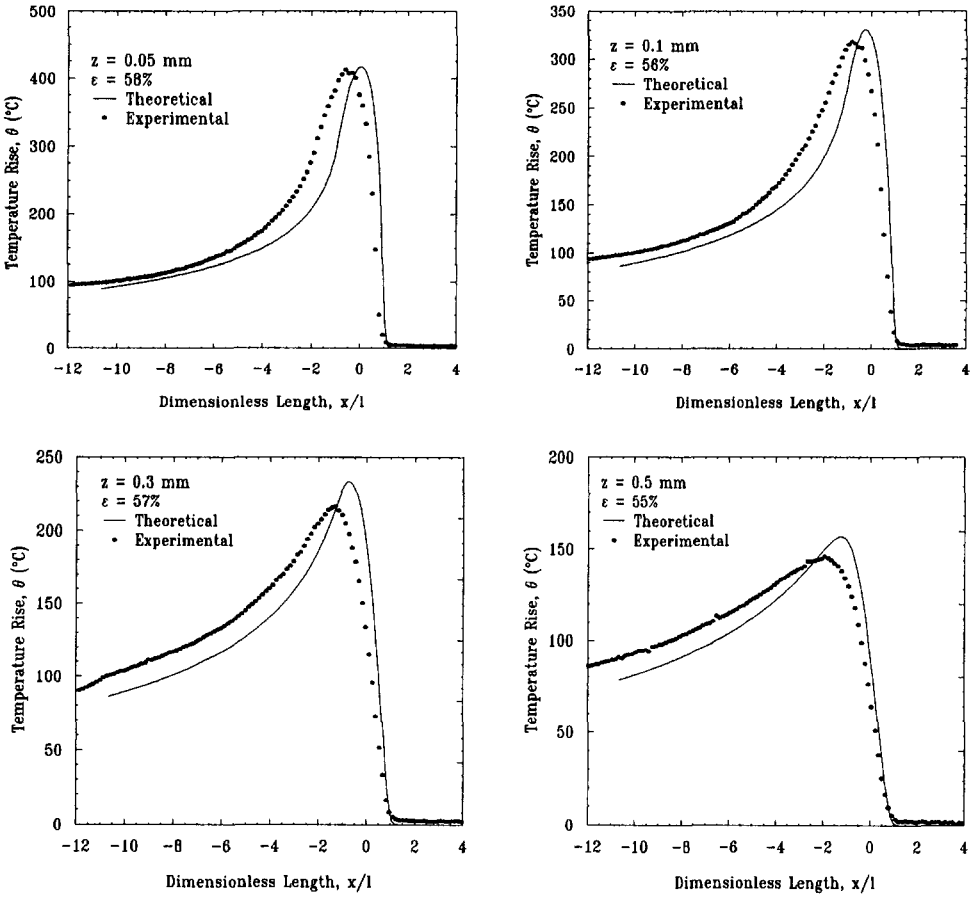

Fig. 3 Experimental and theoretical temperatures and energy partition at various depths: AISI 1020 steel workpiece, aluminum oxide wheel, triangular heat source

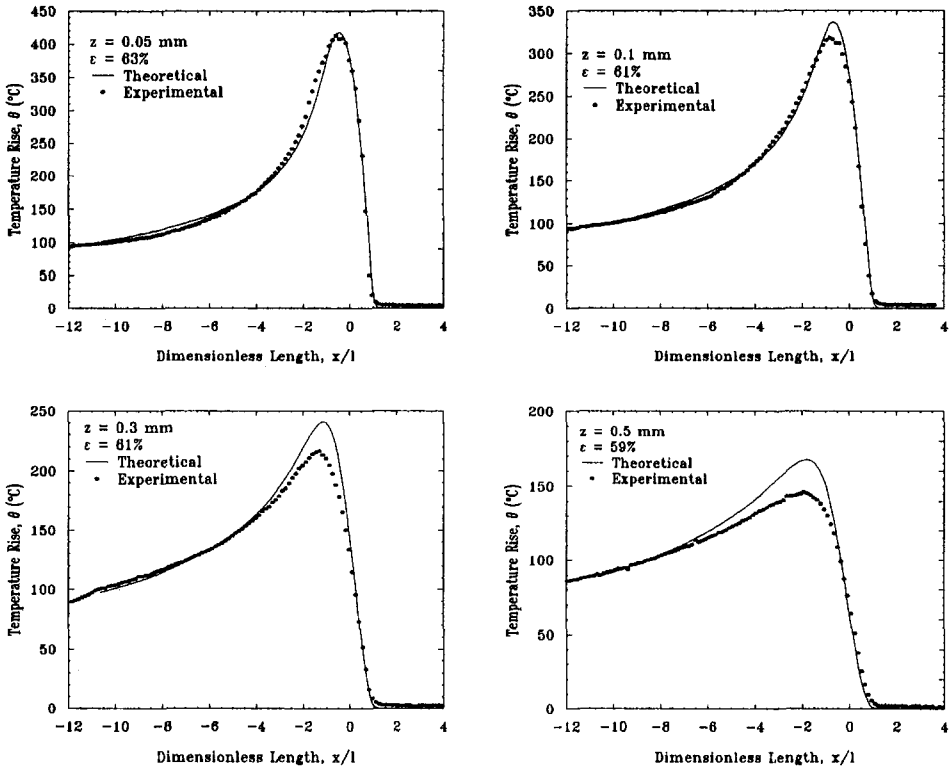

Fig. 4 Experimental and theoretical temperatures and energy partition at various depths: AISI 1020 steel workpiece, aluminum oxide wheel, triangular heat source, time constant τ = 4.3 ms

as first order and a system identification technique utilizing an auto-regression model for parameter estimation was used with the theoretical temperature as input and the experimentally measured data as output. For performing the auto-regression, Matlab[1] routines DTREND and ARX were used. The time constant for the data in Fig. 3 was estimated as τ = 4.3 ms.

Now using this time constant, the temperature from the theoretical model was modified to take the time delay into account using the Matlab[1] simulation routine DLSIM. The theoretical temperature response modified for the time lag is shown together with the experimental data in Fig. 4. By taking the time lag into account, a good in match is obtained between the theoretical and measured temperatures. The measuring system seems to miss some of the temperature peaks, which could be due to the size of the thermocouple. The results indicate that the fraction ϵ of the total grinding energy entering the workpiece as heat is 60 – 65 percent.

Another way to estimate the energy partition is to match the maximum temperatures at different depths for the measured and the theoretical results. In Fig. 5, it can be seen that the maximum temperatures measured at different depths match the corresponding theoretically predicted maximum temperatures from Eq. (2) (corrected for the time delay) fairly well for an energy partition to the workpiece of ϵ = 65 percent. It should be noted that this method might provide a more accurate energy partition estimate than just using a single temperature response.

As previously stated, temperatures in grinding are often calculated using a rectangular heat source distribution (see Fig. 2) instead of a triangular heat source distribution. The theoretical temperature distribution for the rectangular heat source is simply obtained by substituting $f(x')$ = 1 into Eq. (2). It can be seen in Fig. 6 that the triangular heat source gave a much better match between the theoretical and measured temperatures. Therefore, the triangular heat source distribution was used for all the remaining calculations.

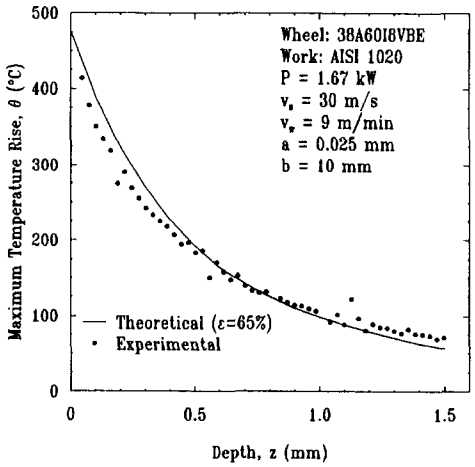

Fig. 5 Experimental and theoretical maximum temperature rise versus depth for energy partition ϵ = 65 percent; AISI 1020 steel workpiece, aluminum oxide wheel, triangular heat source, time constant τ = 4.3 ms

The next experiment was originally intended for grinding the same AISI 1020 plain carbon steel workpiece with the vitrified CBN wheel. However, grinding of this soft steel workpiece with this CBN wheel led to excessive wheel loading even when the applied flow rate of the grinding fluid was increased from its initial low value of 5 ml/s to 40 ml/s. Therefore it was decided to change the workpiece material to hardened AISI 52100 bearing steel, which could be readily ground with both aluminum oxide and CBN abrasive wheels. Experiments were conducted as before and the results analyzed using the

[1]The Mathworks, Inc.

temperature distribution for a triangular heat source modified for a time delay in the system. In this and subsequent tests, the time constant was again found to be very close to 4.3 ms. The results in Fig. 7 with the aluminum oxide indicate that approximately 60–75 percent of the total grinding energy enters the workpiece as heat. Although the results agree fairly well within the grinding zone and ahead of its leading edge, the theoretical temperature behind the trailing edge of the grinding zone is now significantly higher than that obtained experimentally. This may be attributed to cooling by the more intense grinding fluid application. In order to analytically take this effect into account, the thermal analysis was modified by specifying a boundary condition with convective heat transfer on the top surface behind the trailing edge of the heat source where the fluid reaches the workpiece, instead of an insulated surface. The temperature distribution was then numerically calculated using a finite difference method. The theoretical results in Fig. 7 show that cooling behind the trailing edge has virtually no influence on the temperature distribution within the grinding zone. The theoretical and the experimental results agree fairly well for a heat transfer coefficient h = 40,000 W/m^2 K and an energy partition to the workpiece of ϵ = 60–75 percent.

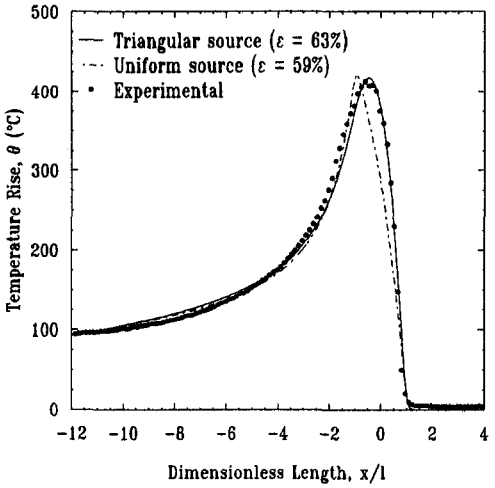

Fig. 6 Comparison of measured and theoretical temperature distributions at depth of 0.05 mm using triangular and rectangular heat sources with a time constant τ = 4.3 ms

In Fig. 8 the maximum temperatures obtained at different depths for the same experiment are plotted together with the corresponding theoretically predicted maximum temperatures to obtain the energy partition. The maximum theoretical temperatures were obtained for convective cooling (h = 40,000 W/m^{2}K) behind the trailing edge with the time delay. When analyzed in this way, the experimental results indicate that approximately 60 percent of the total energy entered the workpiece as heat.

The next experiment was performed using the vitrified CBN wheel on the AISI 52100 steel workpiece. The results are shown in Fig. 9 where it can be seen that only about 20 percent of the total energy entered the workpiece. Again the measured temperature behind the trailing edge was lower than theoretically obtained without cooling, so the analysis was modified to include cooling in this region. The results in Fig. 9 suggest

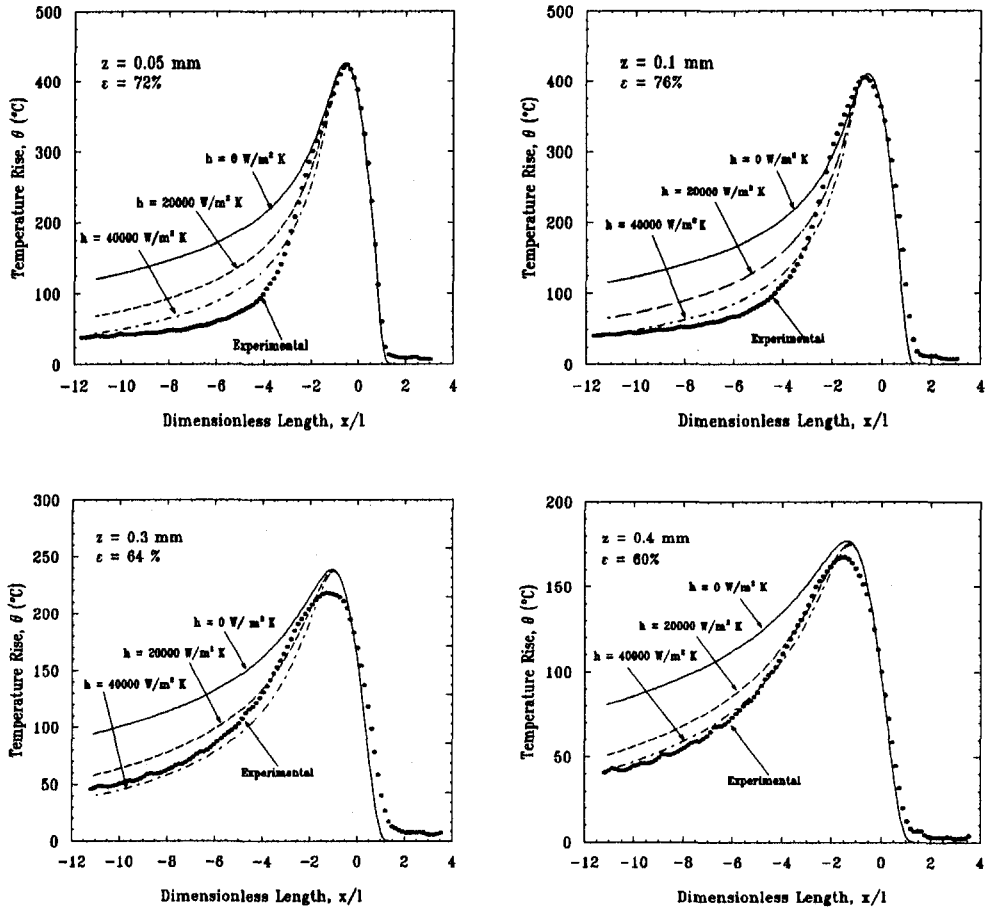

Fig. 7 Experimental and theoretical temperatures and energy partition at various depths: AISI 52100 steel workpiece, aluminum oxide wheel, triangular heat source, time constant τ = 4.3 ms

a convective heat transfer coefficient of about h = 10,000 W/m^2K. Plotting the maximum experimental and theoretical temperatures versus depths in Fig. 10 suggests an energy partition of about 16 percent, which is slightly less than the value of about 20 percent implied in Fig. 9. Clearly the energy partition to the workpiece for the vitrified CBN wheel is much lower than for the aluminum oxide wheel.

The same hardened bearing steel was then ground with the electroplated CBN wheel. These results presented in Fig. 11 indicate an energy partition of about 20 percent and a heat transfer coefficient behind the trailing edge of about h = 15,000 W/m^2 K, which is bigger than what was obtained with the vitrified CBN wheel. It can be seen in Fig. 11 that there is also a slight additional temperature rise ahead of the leading edge, which may be due to hot grinding chips impinging on the workpiece surface. A comparison between the maximum theoretical and experimental temperatures at different depths in Fig. 12 also indicates an energy partition of about 20 percent.

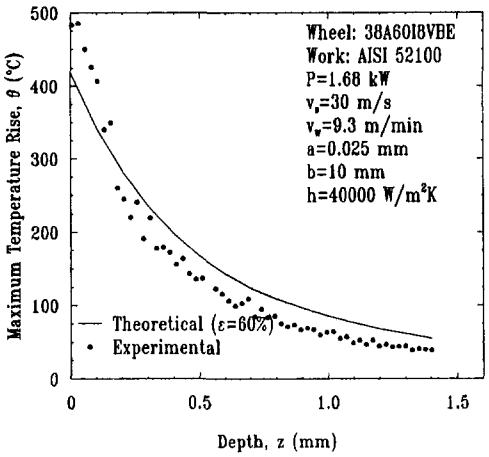

Fig. 8 Experimental and theoretical maximum temperature rise versus depth for energy partition ϵ = 60 percent: AISI 52100 steel workpiece, aluminum oxide wheel, triangular heat source, time constant τ = 4.3 ms

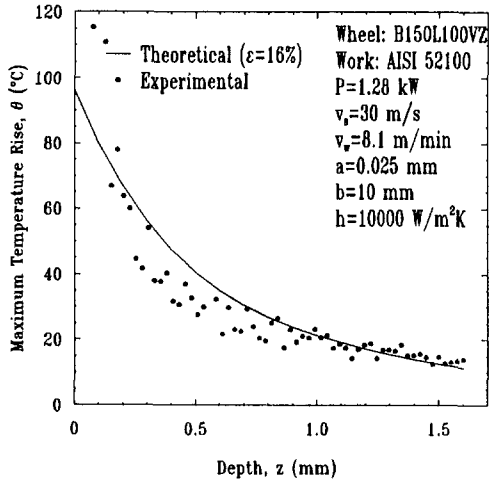

Fig. 10 Experimental and theoretical maximum temperature rise versus depth for energy partition ϵ = 16 percent: AISI 52100 steel workpiece, vitrified CBN wheel, triangular heat source, time constant τ = 4.3 ms

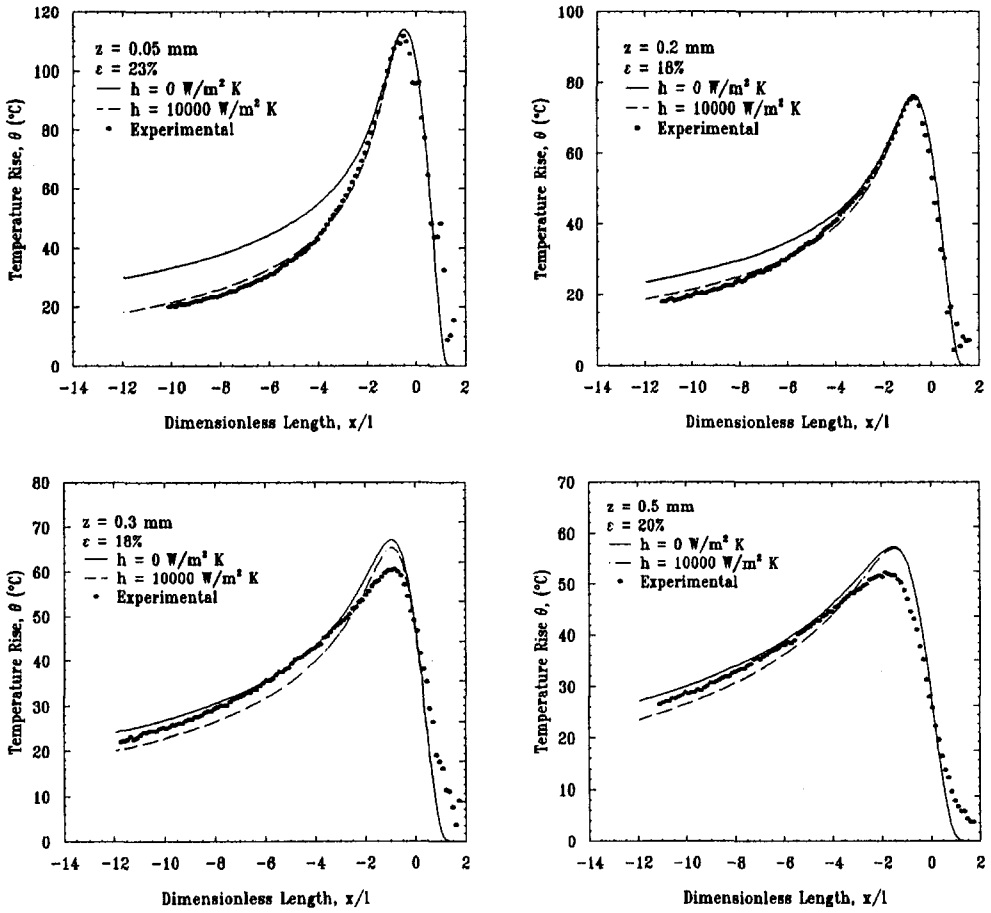

Fig. 9 Experimental and theoretical temperatures and energy partition at various depths: AISI 52100 steel workpiece, vitrified CBN wheel, triangular heat source, time constant τ = 4.3 ms

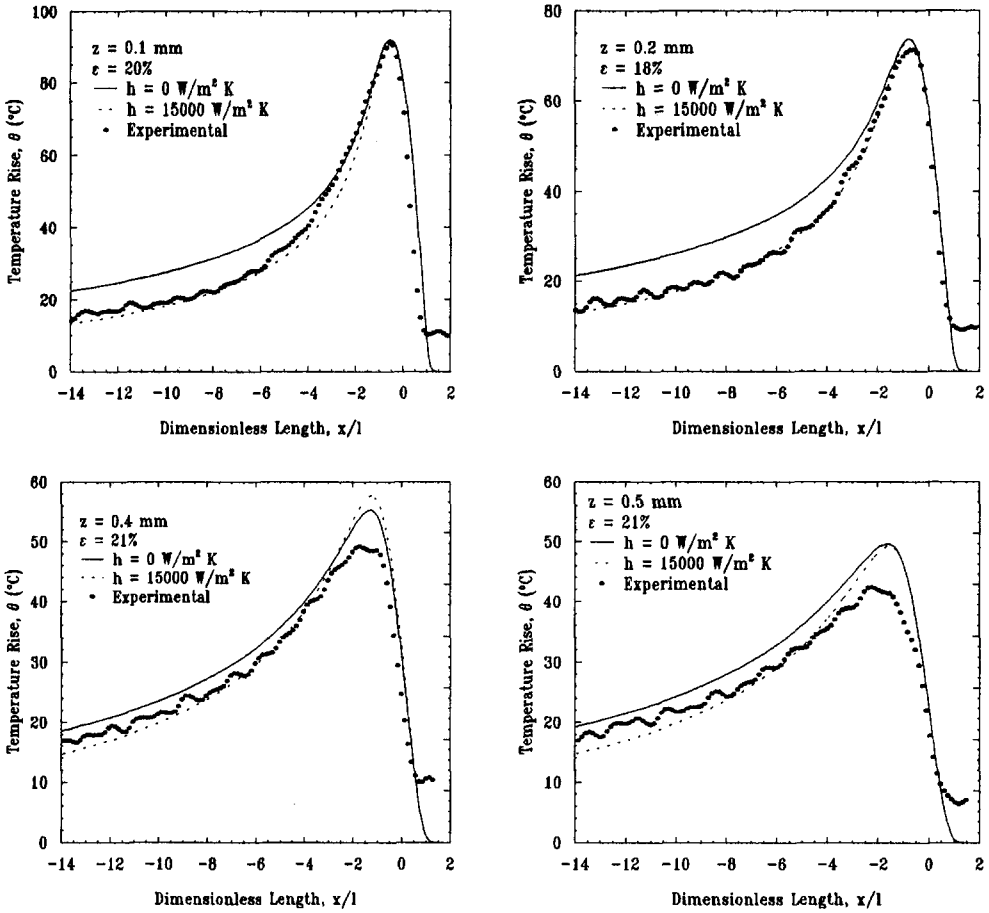

Fig. 11 Experimental and theoretical temperatures and energy partition at various depths: AISI 52100 steel workpiece, electroplated CBN wheel, triangular heat source, time constant τ = 4.3 ms

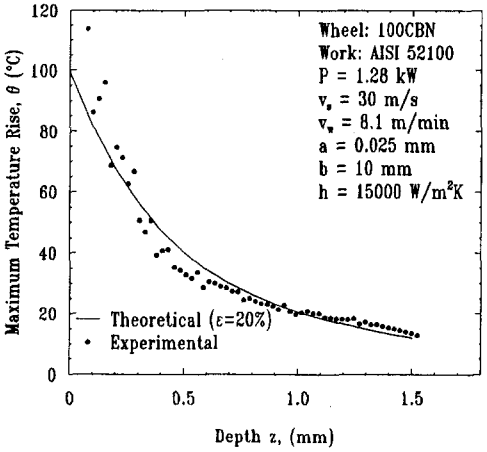

Fig. 12 Experimental and theoretical maximum temperature rise versus depth for energy partition ϵ = 20 percent: AISI 52100 steel workpiece, electroplated CBN wheel, triangular heat source, time constant τ = 4.3 ms

In addition to grinding of bearing steel (AISI 52100) with aluminum oxide and CBN wheels, the energy partition for grinding of a hardened die steel (AISI 01) with the vitrified CBN wheel was also investigated. Experiments were conducted as before and the results analyzed using the triangular heat source modified for the time lag in the system and cooling behind the trailing edge of the grinding zone. The results in Figs. 13 and 14 with h = 15000 W/m^{2}K show good agreement between experimental and theoretical temperatures for an energy partition ϵ = 20 percent.

Discussion

The experimental results indicate that only about 20 percent of the total grinding energy is conducted as heat into the workpiece for grinding with the CBN abrasive wheels versus 60–75 percent for grinding with the conventional aluminum oxide abrasive wheel. Furthermore, a heat source with a triangular heat flux distribution and a source length equal to the geometric contact length was found to provide a good approximation to the thermal situation.

It has been proposed (Kannappan and Malkin, 1972) that the specific grinding energy can be considered to consist of three components: chip formation energy u_{ch} associated with actual material removal, plowing energy u_{pl} associated with workpiece deformation without removal, and sliding energy u_{sl} associated with rubbing between the wear flats and the workpiece:

$$u = u_{ch} + u_{pl} + u_{sl} \tag{4}$$

It was theoretically and experimentally found (Malkin and Anderson, 1974) that nearly all the plowing and sliding energy components are conducted as heat to the workpiece, whereas only about 55 percent of the chip formation energy is conducted as heat to the workpiece, so that:

$$\epsilon = \frac{0.55u_{ch} + u_{pl} + u_{sl}}{u} \tag{5}$$

or combining Eqs. (4) and (5)

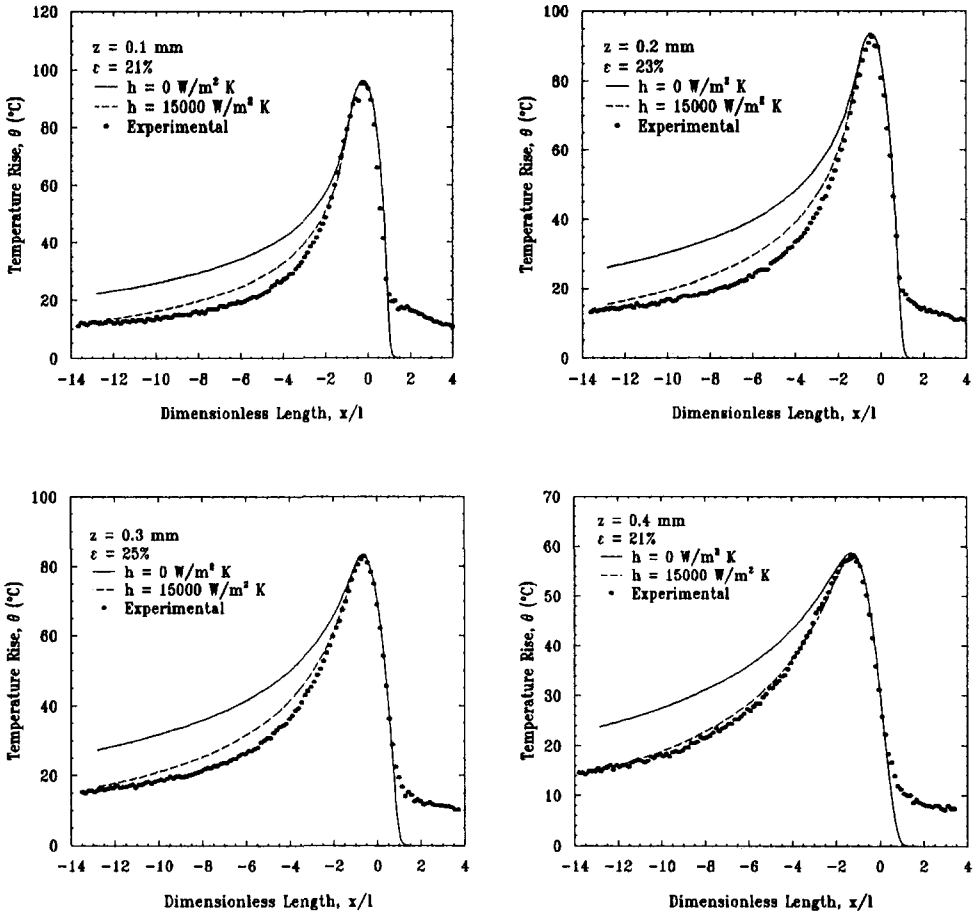

Fig. 13 Experimental and theoretical temperatures and energy partition at various depths: AISI 01 steel workpiece, vitrified CBN wheel, triangular heat source, time constant τ = 4.3 ms

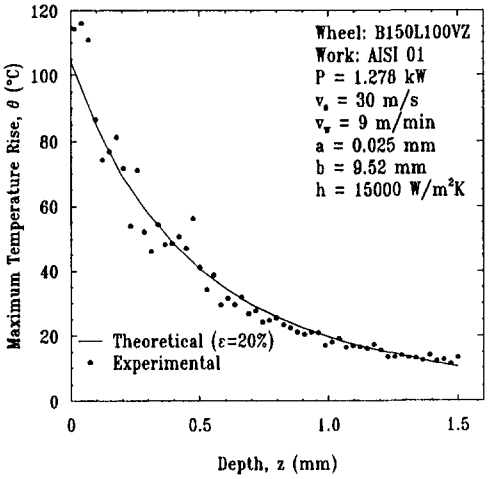

Fig. 14 Experimental and theoretical maximum temperature rise versus depth for energy partition ϵ = 20 percent: AISI 01 steel workpiece, vitrified CBN wheel, triangular heat source, time constant τ = 4.3 ms

$$\epsilon = \frac{u - 0.45u_{ch}}{u} \tag{6}$$

The chip formation energy component u_{ch} is approximately 13.8 J/mm^3 for grinding of steels. For typical grinding conditions, the energy partition obtained from this relationship ranges from 60 percent to 90 percent. For the specific grinding energy u of about 44 J/mm^3 obtained for grinding the AISI 1020 plain carbon steel and AISI 52100 bearing steel with the aluminum oxide wheel, the energy partition according to Eq. (6) would be approximately 85 percent, which is somewhat higher than the measured values. The discrepancy between the predictions of the previous model and the present results may be attributed to a number of factors. First of all, the previous model assumes that all the energy expended by grinding is converted to heat. It has been shown (Taylor and Quinney, 1934) that up to 10 percent of the energy expended by the plastic deformation may not be converted to heat, although for the large strains encountered in machining this may be only 1-3 percent (Shaw, 1984). The previous model also assumes that all the sliding energy due to rubbing between the wear flats and the workpiece is conducted as heat to the workpiece. A closer examination of the friction-slider thermal model for the sliding contact on which the above conclusion was based indicates that about 93 percent of the sliding energy should be conducted to the workpiece and 7 percent to the slider (aluminum oxide grain). Likewise, all the plowing energy associated with deformation of the workpiece material was also assumed to be retained as heat in the workpiece, but the abrasive grains in contact with the workpiece may also conduct away some of this heat. Futhermore the previous model was based on dry grinding conditions, but for wet grinding as used in the present study part of the heat from the grinding zone may be convected away by the coolant. Finally a two dimensional approximation was used for the heat transfer analysis, which neglects the possibility of some heat loss laterally through the sides of the workpiece which would also reduce the measured temperatures.

Much lower temperatures were found for grinding with the CBN abrasive wheels than with the aluminum oxide wheels.

This is partly due to lower specific energies with the CBN wheels (e.g., the specific energy for grinding of AISI 52100 was approximately 35 J/mm^3 with the CBN wheels versus 44 J/mm^3 with the aluminum oxide wheel), but the present results indicate that the difference is mainly due to the much lower fraction of grinding energy entering the workpiece as heat with the CBN abrasive wheels. It has been proposed (Lavine, Malkin and Jen, 1989) that the very high thermal conductivity of the CBN abrasive grain (1300 $Wm^{-1}K^{-1}$ as compared to that of aluminum oxide ($36Wm^{-1}K^{-1}$) can result in a much larger fraction of the heat generated at the wheel workpiece interface being conducted into the abrasive grain instead of into the workpiece. A model was formulated to analyze possible heat conduction to the CBN abrasive grain whereby the grain is approximated as a truncated cone moving along the workpiece surface at the wheel velocity v_s. By equating the maximum temperatures of the workpiece and the grain at their interface, the energy partition to the workpiece is obtained for a triangular heat source distribution as (Guo and Malkin, 1992):

$$\epsilon = \frac{1}{1 + 1.06\left[\frac{\pi(k\rho c)_g v_s}{2(k\rho c)_w v_w}\right]^{1/2} f(\xi) A_0 G_a} \tag{7}$$

where G_a is the number of active grains per unit area of the wheel surface, A_0 the average single grain workpiece contact area corresponding to the truncated area of the cone, k the thermal conductivity, ρc the volumetric specific heat, and the subscripts g and w represent the grain and workpiece, respectively. The value of A_0 corresponding to the measured values of ϵ can be obtained from Eq. (7) with appropriate substitutions. The function $f(\xi)$ takes into account the fact that the grain cross-sectional area is substantially larger than the contact area between the grain and the workpiece and is given by (Lavine, Malkin and Jen, 1989):

$$f(\xi) = \frac{2}{\pi^{1/2}} \frac{\xi}{1 - \exp(\xi^2) erfc(\xi)} \tag{8}$$

where

$$\xi \equiv \left(\frac{\gamma \pi \alpha_g l_c}{2 A_0 v_s}\right)^{1/2} \tag{9}$$

and γ is an abrasive shape factor. Taking typical values $\gamma = 1$, $G_a = 4.34 \times 10^6/m^2$ (150 mesh CBN abrasive, 100 concentration), $(k\rho c)_g = 23 \times 10^8 J^2 s^{-1} m^{-4} K^{-2}$, $(k\rho_c)_w = 2.1 \times 10^8 J^2 s^{-1} m^{-4} K^{-2}$, $\alpha_g = 7.4 \times 10^{-4}$ m^2/s, $l_c = 2.54$ mm, $v_s = 30$ m/s, $v_w = 0.15$ m/s and the experimentally obtained value of $\epsilon = 0.2$, the grain contact area is $A_0 = 1.51 \times 10^{-3}$ mm^2. This area is less than 5 percent of the projected grain area, approximated as a circle of diameter equal to the grain diameter ($\pi d_g^2/4$), which means that only a very small contact area between each active CBN grain and the workpiece is needed to effectively remove heat from the grinding zone.

Conclusions

(1) Approximately 20 percent of the total grinding energy is conducted into the workpiece as heat at the grinding zone for regular grinding with CBN abrasive wheels versus 60-75 percent for grinding with conventional aluminum oxide abrasive wheels. The difference is attributed to the much higher thermal conductivity of the CBN abrasive, whereby a significant portion of the grinding heat is transported to the abrasive instead of the workpiece.

(2) The triangular heat flux distribution within the grinding zone provides a much better approximation to the thermal situation than the rectangular heat flux distribution.

(3) The grinding zone length can be taken as equal to the geometric wheel-workpiece contact length for calculating temperatures in grinding.

(4) Cooling was found to occur mainly behind the trailing edge of the grinding zone where the grinding fluid impinges on the workpiece.

Acknowledgment

This work was supported in part by General Electric Superabrasives. Grinding wheels were supplied by Norton Company and Abrasive Technology, Inc.

References

Guo, C., and Malkin, S., 1992, "Heat Transfer in Grinding," *Journal of Material Processing and Manufacturing Science*, Vol. 1, pp. 16-27.

Jaeger, J. C., 1942, "Moving Sources of Heat and Temperature at Sliding Contact," Proc. Roy. Soc. New South Wales, Vol. 76, pp. 203-224.

Kannappan, S., and Malkin, S., 1972, "Effects of Grain Size and Operating Parameters on the Mechanics of Grinding," ASME JOURNAL OF ENGINEERING FOR INDUSTRY, Vol. 94, pp. 838-842.

Lavine, A. S., and Malkin, S., 1990, "The Role of Cooling in Creep Feed Grinding," *International Journal of Advanced Manufacturing Technology*, Vol. 5, pp. 97-111.

Lavine, A. S., Malkin, S., and Jen, T. C., 1989, "Thermal Aspects of Grinding with CBN Abrasives," *Annals of the CIRP*, Vol. 38, No 1, pp. 557-560.

Littmann, W. E., and Wulff, J., 1955, "The Influence of the Grinding Process on the Structure of Hardened Steel," *Transactions of the ASME*, Vol. 47, pp. 692-714.

Malkin, S., 1989, *Grinding Technology: Theory and Applications of Machining with Abrasives*, Ellis Howard Limited, Chichester and John Wiley & Sons, New York.

Malkin, S., 1985, "Current Trends in CBN Grinding Technology," *Annals of the CIRP*, Vol. 34, No. 2, pp. 557-563.

Malkin, S., and Anderson, R. B., 1974, "Thermal Aspects of Grinding, Part 1-Energy Partition," ASME JOURNAL OF ENGINEERING FOR INDUSTRY, Vol. 96, pp. 1177-1183.

Malkin, S., 1968, *The Attritious and Fracture Wear of Grinding Wheels*, ScD Thesis, MIT.

Maris, M., and Snoeys, R., 1974, "Heat Affected Zone in Grinding Operations," *Proceedings of the 14th International Machine Tool Design and Research Conference*, pp. 659-669.

Sato, K., 1961, "Grinding Temperatures," *Bull. of Japan Society of Grinding Engineers*, Vol. 1, pp. 31-33.

Sauer, W. J., 1971, *Thermal Aspects of Grinding*, Ph.D. Thesis, Carnegie-Mellon University, Pittsburgh, PA.

Shaw, M. C., 1984, *Metal Cutting Principles*, Oxford University Press, London, p. 251.

Snoeys, R., Maris, M., and Peters, J., 1978, "Thermally Induced Damage in Grinding," *Annals of the CIRP*, Vol. 27, No. 2, pp. 571-580.

Takazawa, K., 1966, "Effects of Grinding Variables on Surface Structure of Hardened Steels," *Bull. Japan Soc. Prec. Engg.*, pp. 14-19.

Taylor, G., and Quinney, H., 1934, "The Latent Heat Remaining in a Metal after Cold Working," *Proc. of the Royal Society of London*, Series A, Vol. 143, pp. 307-326.

Tönshoff, H. K., and Hetz, F., 1985, "Influence of Abrasive on Fatigue in Precision Grinding," *Milton C. Shaw Grinding Symposium*, PED-16, ASME, New York, pp. 191-197.

Tönshoff, H. K., and Grabner, T., 1984, "Cylindrical and Profile Grinding with Boron Nitride Wheels," *Proceedings of the 5th International Conference on Production Engineering*, Tokyo, pp. 326-343.

Vansevenant, Ir. E., 1989, "An Improved Mathematical Model to Predict Residual Stresses in Surface Plunge Grinding," *Annals of the CIRP*, Vol. 36, pp. 413-416.